

# Measurement and Correlation of CO<sub>2</sub> Solubility in the Systems of CO<sub>2</sub> + Toluene, CO<sub>2</sub> + Benzene, and CO<sub>2</sub> + *n*-Hexane at Near-Critical and Supercritical Conditions

E. Nemati Lay, V. Taghikhani, and C. Ghotbi\*

Department of Chemical and Petroleum Engineering, Sharif University of Technology, P.O. Box 11365-9465, Azadi Avenue, Tehran, Iran

The solubility of CO<sub>2</sub> in the systems of CO<sub>2</sub> + benzene, CO<sub>2</sub> + *n*-hexane, and CO<sub>2</sub> + toluene was meticulously measured at (293.15, 298.15, and 308.15) K and different pressures using a pressure–volume–temperature (*PVT*) apparatus. Also the effect of pressure on the solubility of CO<sub>2</sub> in the organic solvents used in this work was investigated. The Peng–Robinson equation of state (PR EOS) with only one temperature-independent binary interaction parameter was used in correlating the experimental data. The results showed that the PR EOS can accurately correlate the experimental data for the solubility of CO<sub>2</sub> in the organic solvents at high pressure. In case of the systems CO<sub>2</sub> + benzene and CO<sub>2</sub> + *n*-hexane at 298.15 K, the experimental results obtained from the *PVT* apparatus were compared with those reported in the literature. The comparison showed that for such systems the results are in good agreement with those of previously published experimental data.

## Introduction

Recently supercritical fluid technology has been extensively used in order to produce fine particles. The most important techniques are the rapid expansion solution (RESS) process, the particles from gas-saturated solutions (PGSS) process, the supercritical antisolvent (SAS) recrystallization process, and the gas antisolvent (GAS) process. These versatile techniques have been applied to generate microparticles as well as nanoparticles that can be more importantly used in pharmaceuticals, polymers, biological-active protein, pigments, catalysts, and superconductor industries.<sup>1–5</sup> In the GAS process, a compressed gas or a supercritical fluid is introduced into a solution containing both solvent and solute to be micronized. Due to the volume expansion in the presence of antisolvent, the solvation power decreases, and as a consequence, the solute is compelled to precipitate as fine particles.<sup>6</sup> Although many parameters account for optimizing these processes, it is clear that the phase behavior of such systems can significantly affect the micronization process. The volume expansion of a solvent in the presence of the antisolvent and the solubility of antisolvent (i.e., compressed gas) are two important parameters in the study of the phase behavior of such systems.

The mole fraction of toluene in compressed CO<sub>2</sub> was reported by Prausnitz and Benson<sup>7</sup> at wide temperature range of (323.15 to 348.15) K and in the pressure range of (2 to 9) MPa. Ng and Robinson<sup>8</sup> studied the experimental results for CO<sub>2</sub> + toluene mixtures at temperatures ranging from (311.15 to 477.15) K and at different pressures up to 15 MPa. Sebastian et al.<sup>9</sup> reported vapor–liquid equilibrium data for the CO<sub>2</sub> + toluene system up to 543.15 K and pressure in the range of (1 to 5) MPa. Tochigi et al.<sup>10</sup> studied the vapor–liquid equilibrium for CO<sub>2</sub> + pentane and CO<sub>2</sub> + toluene systems at a temperature

range of (313.15 to 353.15) K and at higher pressure up to 10 MPa.

A number of previous investigations were directed to study the equilibrium phase behavior for the system of CO<sub>2</sub> + benzene. Among them the results presented by Gupta et al.<sup>11</sup> can be mentioned. They reported vapor–liquid equilibrium data at (313.15 to 393.15) K and pressure up to 13.5 MPa. Also Ohgaki and Katayama<sup>12</sup> studied vapor–liquid equilibrium data for CO<sub>2</sub> + benzene and CO<sub>2</sub> + *n*-hexane systems at temperatures of (298.15 and 313.15) K and various pressures up to 8 MPa.

In this work, the solubility of CO<sub>2</sub> in toluene, benzene, and *n*-hexane was measured at (293.15, 298.15, and 308.15) K at different pressures. The results obtained were also correlated using the Peng–Robinson equation of state (PR EOS) with one temperature-independent binary interaction parameter. The values for the binary interaction parameters were reported for each system. It is worth noting that the experiments carried out in this work were replicated three times and that the results presented are the average of the replicates.

## Experimental Section

**Materials.** Benzene, toluene, and *n*-hexane were supplied from Merck Company. The purity of the chemicals was estimated to be 99 % according to the information given by the manufacturer. Carbon dioxide with a purity of 99.99 % was purchased from Air Products Company. All the chemicals were used as received without further purification.

**Apparatus.** A schematic diagram of the pressure–volume–temperature (*PVT*) apparatus (D. B. Robinson Design & Manufacturing Ltd., Edmonton, AB, Canada) is shown in Figure 1. The apparatus is similar to that used by Kho et al.<sup>13</sup> In order to study phase behavior and to measure the solubility of the binary systems of CO<sub>2</sub> + benzene, CO<sub>2</sub> + *n*-hexane, and CO<sub>2</sub> + toluene, an apparatus containing a *PVT* cell was used. The *PVT* apparatus consists of a high accurate temperature-

\* Corresponding author. E-mail: ghotbi@sharif.edu. Tel.: +98 21 6005819. Fax: +98 21 602 2853.

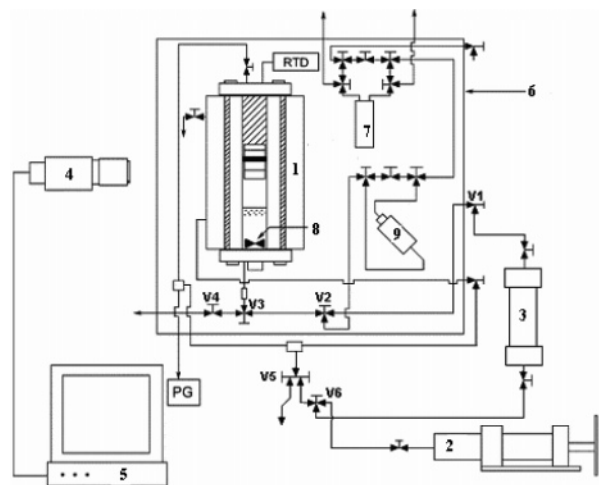


**Figure 1.** Schematic diagram of the PVT apparatus used in this work: 1, high-pressure view cell; 2, high-pressure pump; 3, sample cylinder; 4, CCD camera; 5, video monitor; 6, temperature-controlled bath; 7, densitometer; 8, mixer; 9, in-line viscometer; RTD, resistance temperature detector; PG, pressure gauge.

controlled airbath with an accuracy of  $\pm 0.1$  K that houses a high-pressure variable view cell, with total sample volume of 130 mL rated to 70 MPa and 473.15 K, equipped with a magnetic mixer and a low-volume sampling port. The pressure of the system was measured with a digital pressure indicator, Heise model 901 A, with accuracy of  $\pm 0.05$  MPa. The temperature of the air bath unit and the PVT cell is measured with two platinum 100  $\Omega$  resistance thermocouples with an accuracy of  $\pm 0.3$  K. The volume of the fluid phase in the PVT cell can be measured using a CCD camera-based measurement system with accuracy of  $\pm 0.01$  mL. Pressurization of the PVT cell can be achieved via a computer-controlled, high-pressure positive displacement pump with a volume resolution of 0.01 mL. The apparatus also features a high-pressure densitometer (Anton Paar, model DMA 512P) rated up to 70 MPa and 423.15 K and an in-line electromagnetic viscometer (Cambridge Applied Systems, Medford, MA; model SPL440) rated up to 140 MPa and 463.15 K, with viscosity range of 0.1 to 10 000 cP.

For the solubility measurements of carbon dioxide in the solvents studied in this work, a 10 L gasometer (D. B. Robinson Design & Manufacturing Ltd.) with 0.1 cm<sup>3</sup> resolution was used for accurate measurement of gas volume at atmospheric pressure. The apparatus was also connected with the real-time data acquisition system. The data acquisition system not only supports all the standard instruments in the PVT apparatus including pressure, temperature, volume, density, and viscosity measurements but also provides a full control system for the pumping operation.

**Procedure.** Before beginning the experiments, the lines, sample cylinder, and PVT cell were cleansed, dried, and evacuated. Then the sample cylinder was charged by desired solvent. Ten millimeters of solvent in each experimental run was injected into the evacuated view cell. Then a sufficient amount of CO<sub>2</sub> was introduced into the view cell, and the solution was mixed vigorously using the magnetic mixer. Having reached the thermodynamic equilibrium condition, as indicated by the pressure and temperature of the view cell, a known amount of liquid-phase sample was charged into the evacuated and balanced standard bomb (S.S.316, 75.0 mL volume, rated up to 12 MPa) through the sampling valve. The charging process was done slowly to avoid flushing. The charged liquid sample was weighted using a balance with the accuracy of  $\pm 1$  mg.

Sampling and balancing the liquid phase, the bomb was connected to the evacuated gasometer for measuring the volume of gaseous CO<sub>2</sub> at atmospheric pressure. Also solvent was directly trapped into the cooling trap. Neglecting the vapor pressure of the pure organic liquid, the quantity of the dissolved gas in the solvents was measured volumetrically. The CO<sub>2</sub> solubility in the organic solvent can be given by the following relation:

$$X_{\text{CO}_2} = \frac{m_{\text{CO}_2}}{m_s} = \left( \frac{P \text{VMW}_{\text{CO}_2}}{zRT} \right) / m_s \quad (1)$$

where  $R$  is the universal gas constant,  $V$  is the amount of gas released including the calibrated dead volume at atmospheric pressure and at the desired temperature,  $MW$  is the molecular weight of CO<sub>2</sub>, and  $m_s$  is the total amount of sample that exists in the bomb. The ideal gas behavior for vapor phase was assumed at atmospheric pressure. The mole fraction and solubility of CO<sub>2</sub> in the organic solvents can be calculated from the measured mass fraction.

**Modeling.** The PR EOS was used to correlate the VLE data obtained in this work.<sup>14</sup> The PR EOS can be given by the following equation:

$$P = \frac{RT}{v-b} - \frac{a}{v(v+b) + b(v-b)} \quad (2)$$

The parameters of the PR EOS can be obtained using the following quadratic mixing rules:

$$a = \sum_i^n \sum_j^n x_i x_j \sqrt{a_i a_j} (1 - \delta_{ij}) \quad (3)$$

and

$$b = \sum_i^n x_i b_i \quad (4)$$

where  $x_i$  is the mole fraction or solubility of component  $i$  and  $\delta_{ij}$  is the binary interaction parameter for an  $i$ - $j$  pair.

**Table 1.** Experimental Mole Fraction Solubility of CO<sub>2</sub> ( $x_1$ ) in Benzene, *n*-Hexane, and Toluene at (293.15, 298.15, and 308.15) K

$P$ MPa	$T/K$			$P$ MPa	$T/K$		
	293.15	298.15	308.15		293.15	298.15	308.15
$x_1$ , CO <sub>2</sub> + Benzene							
1.70	0.230	0.210	0.179	4.76	0.852	0.715	0.534
2.21	0.309	0.282	0.233	5.27	0.979	0.821	0.645
2.72	0.383	0.341	0.297	5.78		0.965	0.715
3.23	0.477	0.421	0.363	6.29			0.827
3.74	0.578	0.510	0.413	6.80			0.945
4.25	0.704	0.601	0.471	7.31			0.971
CO <sub>2</sub> + <i>n</i> -Hexane							
1.70	0.250	0.238	0.217	4.76	0.882	0.775	0.594
2.21	0.329	0.301	0.280	5.27	0.945	0.855	0.711
2.72	0.421	0.373	0.332	5.78		0.963	0.795
3.23	0.503	0.454	0.401	6.29			0.887
3.74	0.586	0.543	0.475	6.80			0.915
4.25	0.711	0.619	0.529	7.31			0.971
CO <sub>2</sub> + Toluene							
1.70	0.215	0.208	0.180	5.27	0.941	0.795	0.584
2.21	0.281	0.273	0.230	5.78			0.666
2.72	0.353	0.339	0.279	5.92		0.945	
3.23	0.439	0.418	0.335	6.29			0.768
3.74	0.519	0.472	0.411	6.80			0.884
4.25	0.625	0.578	0.457	7.31			0.955
4.76	0.765	0.671	0.535				

**Table 2. Correlated Liquid-Phase Mole Fraction of CO<sub>2</sub> (x<sub>1</sub>) and Vapor-Phase Mole Fraction of CO<sub>2</sub> (y<sub>1</sub>) for the Binary Systems of CO<sub>2</sub> + Benzene, CO<sub>2</sub> + *n*-Hexane, and CO<sub>2</sub> + Toluene at (293.15, 298.15, and 308.15) K**

CO <sub>2</sub> + Benzene						
<i>P</i>	<i>T</i> = 293.15 K		<i>T</i> = 298.15 K		<i>T</i> = 308.15 K	
	δ <sub>ij</sub> = 0.08		δ <sub>ij</sub> = 0.08		δ <sub>ij</sub> = 0.08	
MPa	x <sub>1</sub>	y <sub>1</sub>	x <sub>1</sub>	y <sub>1</sub>	x <sub>1</sub>	y <sub>1</sub>
1.70	0.232	0.9920	0.213	0.9899	0.181	0.9846
2.21	0.307	0.9933	0.280	0.9916	0.236	0.9872
2.72	0.386	0.9941	0.349	0.9926	0.293	0.9888
3.23	0.472	0.9947	0.423	0.9933	0.351	0.9897
3.74	0.570	0.9950	0.503	0.9937	0.411	0.9903
4.25	0.693	0.9953	0.594	0.9939	0.474	0.9906
4.76	0.843	0.9958	0.705	0.9941	0.542	0.9908
5.27	0.951	0.9972	0.838	0.9945	0.617	0.9908
5.78			0.939	0.9956	0.706	0.9907
6.29					0.809	0.9905
6.80					0.905	0.9907
7.31					0.964	0.9916
AARD %	1.28		1.52		1.87	

CO <sub>2</sub> + <i>n</i> -Hexane						
<i>P</i>	<i>T</i> = 293.15 K		<i>T</i> = 298.15 K		<i>T</i> = 308.15 K	
	δ <sub>ij</sub> = 0.11		δ <sub>ij</sub> = 0.11		δ <sub>ij</sub> = 0.10	
MPa	x <sub>1</sub>	y <sub>1</sub>	x <sub>1</sub>	y <sub>1</sub>	x <sub>1</sub>	y <sub>1</sub>
1.70	0.253	0.9870	0.235	0.9839	0.214	0.9761
2.21	0.331	0.9891	0.306	0.9865	0.278	0.9799
2.72	0.412	0.9902	0.379	0.9879	0.342	0.9822
3.23	0.498	0.9909	0.455	0.9888	0.406	0.9836
3.74	0.593	0.9914	0.536	0.9893	0.472	0.9844
4.25	0.708	0.9918	0.625	0.9896	0.539	0.9849
4.76	0.849	0.9926	0.731	0.9899	0.611	0.9851
5.27	0.951	0.9950	0.853	0.9905	0.687	0.9850
5.78			0.942	0.9926	0.771	0.9849
6.29					0.857	0.9849
6.80					0.925	0.9855
7.31					0.969	0.9875
AARD %	1.37		1.68		1.90	

CO <sub>2</sub> + Toluene						
<i>P</i>	<i>T</i> = 293.15 K		<i>T</i> = 298.15 K		<i>T</i> = 308.15 K	
	δ <sub>ij</sub> = 0.10		δ <sub>ij</sub> = 0.09		δ <sub>ij</sub> = 0.09	
MPa	x <sub>1</sub>	y <sub>1</sub>	x <sub>1</sub>	y <sub>1</sub>	x <sub>1</sub>	y <sub>1</sub>
1.70	0.217	0.9975	0.212	0.9968	0.182	0.9949
2.21	0.283	0.9978	0.275	0.9973	0.236	0.9956
2.72	0.352	0.9980	0.341	0.9975	0.290	0.9960
3.23	0.425	0.9981	0.408	0.9976	0.344	0.9962
3.74	0.506	0.9981	0.479	0.9976	0.399	0.9963
4.25	0.602	0.9981	0.557	0.9976	0.456	0.9963
4.76	0.751	0.9980	0.650	0.9975	0.516	0.9962
5.27	0.947	0.9984	0.780	0.9974	0.580	0.9960
5.78					0.653	0.9957
5.92			0.954	0.9978		
6.29					0.746	0.9953
6.80					0.875	0.9947
7.31					0.962	0.9946
AARD %	1.72		1.86		2.02	

The average absolute relative deviation percent (AARD %) was minimized to obtain the values of the binary interactions according to the following equation:

$$\text{AARD \%} = \left( \frac{\sum_i^N \left| \frac{X_i^{\text{exp}} - X_i^{\text{cal}}}{X_i^{\text{exp}}} \right|}{N} \right) \times 100 \quad (5)$$

where *N* is the number of experimental points. The superscripts

exp and cal denote the experimental and calculated values, respectively.

## Results and Discussion

Table 1 reports the values for solubility of CO<sub>2</sub> (x<sub>1</sub>) in the systems of CO<sub>2</sub> + benzene, CO<sub>2</sub> + *n*-hexane, and CO<sub>2</sub> + toluene measured at (293.15, 298.15, and 308.15) K and at various pressures. As can be seen from Table 1, the solubility of CO<sub>2</sub> in the organic solvents increases as the pressure of the system increases. The increase in solubility can be significant using near-critical CO<sub>2</sub>. Such trends can be observed for all systems studied in this work. Table 1 also shows that the solubility of CO<sub>2</sub> can be much affected by the nature of the organic solvents and by system temperature. It is worth mentioning that the experiments were replicated three times, and the results are the average of the replicates. The reproducibility of the CO<sub>2</sub> solubility at constant temperature and pressure was to be found out to be within ± 1.3 %, and the estimated uncertainty<sup>15</sup> of the measurements was less than 2.1 %.

Table 2 presents the results for the mole fraction of CO<sub>2</sub> in liquid and vapor phases respectively obtained from the well-known cubic equation of state, the PR EOS with one binary interaction parameter, along with the grand AARD % of the PR EOS from the experimental data. A careful study of Tables 1 and 2 reveals that the results obtained from the PR EOS can accurately correlate the experimental solubility data at different pressures. It should be stated that the binary interaction parameter was considered to be adjustable parameter in correlating the experimental data using the PR EOS and that the values for the binary interaction parameters at different pressures for each specified system were reported.

The correlated vapor-phase mole fraction of CO<sub>2</sub> for the systems of CO<sub>2</sub> + benzene and CO<sub>2</sub> + *n*-hexane was compared with those reported by Ohgaki and Katayama<sup>12</sup> at 298.15 K. The percent of AARDs of vapor-phase mole fraction of CO<sub>2</sub> in benzene and *n*-hexane at 298.15 K are 0.09 % and 0.39 % respectively.

## Conclusions

Solubility of CO<sub>2</sub> in toluene, benzene, and *n*-hexane were measured at (293.15, 298.15, and 308.15) K and pressures up to 7.5 MPa. The PR EOS with only one interaction parameter was used in correlating the experimental data generated in this work. The results showed that the PR EOS can accurately correlate the experimental data for the solubility of CO<sub>2</sub> in the organic solvents at high pressure.

The results showed that carbon dioxide can be dissolved readily in benzene, *n*-hexane, and toluene at elevated pressures. At 293.15 K and at pressures higher than 4 MPa, the liquid phase contains mostly carbon dioxide, and such behavior can be observed at higher pressure with increasing temperature. These conditions are considered to be appropriate in the GAS process.

## Literature Cited

- (1) Matson, D. W.; Fulton, J. L.; Petersen, R. C.; Smith, R. D. Rapid expansion of supercritical fluid solutions: solute formation of powders, thin film and fibers. *Ind. Eng. Chem. Res.* **1987**, *26*, 2298–2306.
- (2) Chattopadhyay, P.; Gupta, R. B. Production of antibiotic nanoparticles using supercritical CO<sub>2</sub> as antisolvent with enhanced mass transfer. *Ind. Eng. Chem. Res.* **2001**, *40*, 3530–3539.
- (3) Kikic, I.; Lora, M.; Bertucco, A. Thermodynamic analysis of three-phase equilibria in binary and ternary systems for applications in rapid expansion of a supercritical solution (RESS), particles from gas-saturated solutions (PGSS) and supercritical antisolvent crystallization (SAS). *Ind. Eng. Chem. Res.* **1997**, *36*, 5507–5515.

- (4) Cocero, M. J.; Ferrero, S. Crystallization of  $\beta$ -carotene by a GAS process in batch: effect of operating parameters. *J. Supercrit. Fluids* **2002**, *22*, 237–245.
- (5) Kalogiannis, C. G.; Eleni, P.; Panayiotou, C. G. Production of amoxicillin microparticles by supercritical antisolvent precipitation. *Ind. Eng. Chem. Res.* **2005**, *44*, 9339–9346.
- (6) de la Fuente, J. C.; Peters, C. J.; de Swaan Aronsq, J. Volume expansion in relation to the gas antisolvent process. *J. Supercrit. Fluids* **2000**, *17*, 13–23.
- (7) Prausnitz, J. M.; Benson, P. R. Solubility of liquids in compressed hydrogen, nitrogen and carbon dioxide. *AIChE J.* **1959**, *5*, 161–164.
- (8) Ng, H. J.; Robinson, D. B. Equilibrium phase properties of the toluene/carbon dioxide system. *J. Chem. Eng. Data* **1978**, *23*, 325–327.
- (9) Sebastian, H. M.; Simnick, J. J.; Lin, H. M.; Chao, K. C. Gas–liquid equilibrium in mixture of carbon dioxide/toluene and carbon dioxide/*m*-xylene. *J. Chem. Eng. Data* **1980**, *25*, 246–248.
- (10) Tochigi, K.; Hasegawa, K.; Asano, N.; Kojima, K. Vapor–liquid equilibria for the carbon dioxide/pentane and carbon dioxide/toluene systems. *J. Chem. Eng. Data* **1998**, *43*, 954–956.
- (11) Gupta, M. K.; Li, Y. H.; Huisey, B. J.; Robinson, R. L., Jr. Phase equilibrium for carbon dioxide/benzene at 313.2, 353.2, and 393.2 K. *J. Chem. Eng. Data* **1982**, *27*, 55–57.
- (12) Ohgaki, K.; Katayama, T. Isothermal vapor–liquid equilibrium data for binary systems containing carbon dioxide at high pressures: carbon dioxide/methanol, carbon dioxide/*n*-hexane, and carbon dioxide/benzene systems. *J. Chem. Eng. Data* **1976**, *21*, 53–55.
- (13) Kho, Y. W.; Conrad, D. C.; Knutson, B. L. Phase equilibria and thermophysical properties of carbon dioxide–expanded fluorinated solvents. *Fluid Phase Equilib.* **2003**, *206*, 179–193.
- (14) Peng, D.; Robinson, D. B. A new two-constant equation of state. *Ind. Eng. Chem. Fundam.* **1976**, *5*, 59–64.
- (15) Taylor, B. N.; Kuyatt, C. E. *Guidelines for the Evaluation and Expression of Uncertainty in NIST Measurement Results*; NIST Technical Note 129; National Institute of Standards and Technology: Gaithersburg, MD, 1994.

Received for review June 28, 2006. Accepted August 8, 2006.

JE0602972